The current issue and full text archive of this journal is available on Emerald Insight at:
https://www.emerald.com/insight/0961-5539.htm

Exploration of particle shape effect on Cu-H_2O nanoparticles over a moving plate

An approach of dual solution

Ganesh Kumar K.
Department of Studies and Research in Mathematics, Kuvempu University, Shimoga, Karnataka, India

Chamkha Ali J.
Department of Mechanical Engineering, Prince Mohammad Bin Fahd University, Al-Khobar, Saudi Arabia

Prasannakumara B.C.
Department of PG Studies and Research in Mathematics, Davanagere University, Davanagere, Karnataka, India, and

Jyothi A.M.
Department of Mathematics, Bangalore Institute of Technology, Bangalore, India

Received 1 October 2018
Revised 28 November 2018
Accepted 7 December 2018

Abstract

Purpose – This paper aims to explore particle shape effect on Cu-H_2O nanoparticles over a moving plate in the presence of nonlinear thermal radiation. To characterize the effect, particle shape and viscous dissipation are considered. Convergent solutions for the resulting nonlinear systems are derived and the effects of embedded parameters of interest on velocity and temperature field are examined.

Design/methodology/approach – The Runge–Kutta–Fehlberg fourth-fifth order method along with shooting technique is used to solve the governing equations (6) and (7) with boundary conditions (8). A suitable finite value of η_∞ is considered in such a way that the boundary conditions are satisfied asymptotically.

Findings – The results show an increase in both the heat transfer and thermodynamic performance of the system. However, among the three nanoparticle shapes, disk shape exhibited better heat transfer characteristics and heat transfer rate. On the other hand, the velocity profile enhances with increasing values of ϕ in the first solution, but the opposite trend was found in the second solution.

Originality/value – The present paper deals with an exploration of particle shape effect on Cu-H_2O nanoparticles over a moving plate in the presence of nonlinear thermal radiation. To characterize the effect, particle shape and viscous dissipation are considered. Convergent solutions for the resulting nonlinear systems are derived and the effects of embedded parameters of interest on velocity and temperature field are examined. The skin friction coefficient and Nusselt number are numerically tabulated and discussed. The results show an increase in both heat transfer and thermodynamic performance of the system. However, among the three nanoparticle shapes, disk shape exhibited better heat-transfer characteristics and heat-transfer rate. On the other hand, the velocity profile enhances with increasing values of ϕ in the first solution, but the opposite trend was found in the second solution.

Keywords Viscous dissipation, Dual solution, Nonlinear thermal radiation, Particle shape effect

Paper type Research paper

International Journal of Numerical Methods for Heat & Fluid Flow
Vol. 30 No. 4, 2020
pp. 1867-1879

0961-5539
DOI 10.1108/HFF-10-2018-0539

Introduction

Many experimental and theoretical studies have addressed the effect of particle shape on nanofluid flows. Nanomaterials are widely incorporated in numerous engineering areas, including solar collectors, electronics, optics, catalysis, materials, smart computers, solar cells and renewable energy. The main goal of using nanomaterials in such processes is to augment heat-transfer capability so as to achieve better thermal performance. In view of these applications, Xie *et al.* (2012) discussed the thermal conductivity enhancement of suspensions containing nano-sized alumina particles. Timofeeva *et al.* (2009) compared experimental data with theoretical modeling to discuss particle shape effects on the thermophysical properties of alumina nanoparticles. Lin *et al.* (2016) considered spherical, hexahedron, tetrahedron, columnar and lamina-shaped copper nanoparticles, with water as a base fluid, to study the effect of radiation with exponential temperature on Marangoni boundary-layer flow. Considerable literature is available on these topics (Ellahi *et al.*, 2016; Ellahi *et al.*, 2016; Ooi and Popov, 2013; Trodi and Hocine Benhamza, 2016; Sheikholeslami and Shehzad, 2018; Waqas *et al.*, 2018; Rauf *et al.*, 2017; Sheikholeslami *et al.*, 2018; Sheikholeslami and Shehzad, 2017; Hayat *et al.*, 2017; Upadhya *et al.*, 2018; Ramesh *et al.*, 2015; Ramesh *et al.*, 2017).

The problem of boundary-layer flow on a moving plate is a classic problem, and it has been considered by many researchers. For example, Norfifah *et al.* (Bachok *et al.*, 2010, 2012) discussed the boundary layer flow of nanofluids over a moving surface in a flowing fluid. Turkyilmazoglu (2013) analyzed the unsteady convection flow of some nanofluids past a moving vertical flat plate with heat transfer. Thumma *et al.* (Hussain *et al.*, 2017) studied the magnetohydrodynamics natural convective flow of nanofluids past stationary and moving inclined porous plates, considering temperature and concentration gradients with suction. The topic of boundary-layer flow on a moving plate has been surveyed in various review articles (Ma *et al.*, 2017; Kadiyala and Chattopadhyay, 2018; Gul *et al.*, 2017).

The effects of thermal radiation on flow and heat transfer processes have been attracting researchers because of its applications, which include turbid water bodies, nuclear power plants, gas turbines, the various propulsion devices for aircraft, furnace design, fluidized bed heat exchangers, solar ponds, combustion, solar collectors, photo chemical reactors, missiles, satellites and space vehicles. In view of these applications, Cortell (2014) discussed fluid flow and radiative nonlinear heat transfer over a stretching sheet. Shehzad *et al.* (2014) investigate the three-dimensional flow of Jeffrey nanofluid by considering nonlinear thermal radiation. Hayat *et al.* (2015) studied the three-dimensional flow of viscoelastic nanofluid in the presence of nonlinear thermal radiation. Similar studies of thermal radiation effects can also be seen in Makinde and Animasaun (2016), Kumar *et al.* (2017); Khan *et al.* (2017), Rudraswamy *et al.* (2016); Kumar *et al.* (2018), Ramesh *et al.* (2012); and Grubka and Bobba (1985).

Many authors have studied the flow and heat transfer structures of nanofluids with differently shaped and sized nanoparticles. However, these deal for the most part with spherical nanoparticles and the flow regime over a stretched surface. To the best of the authors' knowledge, there has been no theoretical investigation of the effect of particle shape on the thermophysical, heat transfer and thermodynamic performance of nanofluid flow over a moving plate. Therefore, the aim of the present study is to study the fluid's movement over a moving plate. Furthermore, a dual solution is obtained for the case when the plate moves in the opposite direction to the free stream. The results for the velocity and temperature profile, skin friction coefficient and local Nusselt number have been considered for varying values of the parameters. The physical features of pertinent parameters are discussed through graphs.

Mathematical formulation

Consider a steady, laminar, two-dimensional boundary-layer flow and heat transfer of a copper–water nanofluid over a moving flat plate with constant velocity U_w, in the same or opposite direction to the free stream U_∞ (Figure 1). The sheet coincides with the plane $y = 0$ and the flow is confined to $y > 0$. The ambient fluid temperature is a constant T_∞. The fluid is water-based with Cu nanoparticles. Three different types of nanoparticle shapes, i.e. sphere, needle and disk, are taken into account in this study. Moreover, it is assumed that the nanoparticles are in thermal equilibrium state. The Rosseland approximation for radiation is considered.

Under the usual boundary-layer approximations, the flow-governing equations of nanofluid are given by:

$$\frac{\partial u}{\partial x} + \frac{\partial v}{\partial y} = 0, \tag{1}$$

$$u\frac{\partial u}{\partial x} + v\frac{\partial u}{\partial y} = \frac{\mu_{nf}}{\rho_{nf}}\frac{\partial^2 u}{\partial y^2}, \tag{2}$$

$$(\rho c_p)_{nf}\left[u\frac{\partial T}{\partial x} + v\frac{\partial T}{\partial y}\right] = \frac{\partial}{\partial y}\left[\left(k_{nf} + \frac{16\sigma^* T^3}{3k^*}\right)\frac{\partial T}{\partial y}\right] + \left(\frac{\partial u}{\partial y}\right)^2 \tag{3}$$

where x and y, respectively, represent the coordinate axis along the continuous surface in the direction of motion and perpendicular to it. The velocity components of the nanofluid along the x and y directions are denoted by u and v, respectively. $K = 6\pi\mu_{nf}r$ is Stokes' drag constant, r is the radius of dust particle, σ is the electrical conductivity, ρ_{nf} is effective density of nanofluid and μ_{nf} is effective dynamic viscosity of nanofluid, which are given by:

$$\rho_{nf} = (1-\phi)\rho_f + \phi\rho_s, \mu_{nf} = \frac{\mu_f}{(1-\phi)^{2.5}},$$

where ϕ is solid volume fraction of nanofluid, ρ_f is the density of base fluid, ρ_s is the density of nanoparticles and μ_f is the dynamic viscosity of the base fluid.

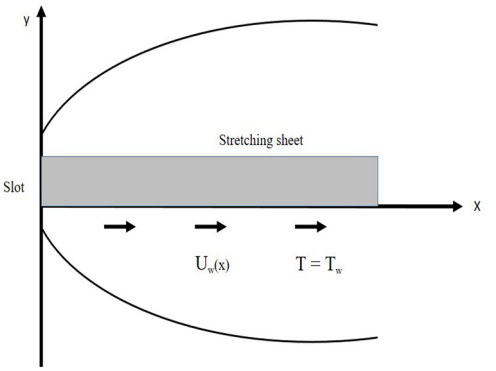

Figure 1.
Physical geometry of the problem

In equation (3), T is the temperatures of the fluid particles inside the boundary layer, c_{pf} is the specific heat of the fluid particles, σ^* is the Stefan–Boltzmann constant, k^* is the mean absorption coefficient, q_r is the radiative heat flux, k_{nf} is the thermal conductivity and $(\rho c_p)_{nf}$ is the heat capacity of the nanofluid, which are given by:

$$\frac{k_{nf}}{k_f} = \frac{\left[k_s + (m-1)k_f\right] - (m-1)\phi\left(k_f - k_s\right)}{\left[k_s + (m-1)k_f\right] + \phi\left(k_f - k_s\right)}, \quad (\rho c_p)_{nf} = (1-\phi)(\rho c_p)_f + (\rho c_p)_s,$$

where $(\rho c_p)_f$ is the heat capacity of the base fluid, $(\rho c_p)_s$ is the heat capacity of nanoparticle, k_f is the thermal conductivity of base fluid and k_s is the thermal conductivity of nanoparticle and m is the particle shape.

The corresponding boundary conditions are given by:

$$\begin{aligned} &u = U_w,\ v = 0, \quad T = T_w \quad \text{at } y = 0, \\ &u \to U_\infty,\ T \to T_\infty \quad \text{as } y \to \infty \end{aligned} \tag{4}$$

To convert the governing equations into a set of similarity equations, the following similarity transformation is introduced:

$$u = Uf'(\eta), \quad v = \sqrt{\frac{\nu_f U}{2x}}\left(\eta f'(\eta) - f(\eta)\right), \quad T = T_w\left(1 + (\theta_w - 1)\theta(\eta)\right),$$
$$\eta = \sqrt{\frac{U}{2\nu_f x}}y, \tag{5}$$

where $U = U_w + U_\infty$, $\theta_w = \frac{T_\infty}{T_w}$, $\theta_w > 1$ the temperature ratio parameter.

Making use of the transformations in equation (5), equation (1) is identically satisfied, and equations (2) and (3) take the form:

$$f''' + (1-\phi)^{2.5}\left[(1-\phi) + \phi\frac{\rho_s}{\rho_f}\right]ff'' = 0, \tag{6}$$

$$\frac{k_{nf}}{k_f}R\left[(1 + (\theta_w - 1)\theta)^3\theta'' + 3(\theta_w - 1)\theta'^2(1 + (\theta_w - 1)\theta)^2\right]$$
$$+ Pr\left[(1-\phi) + \phi\frac{(\rho c_p)_s}{(\rho c_p)_f}\right]\left(f\theta' + Ecf''^2\right) = 0. \tag{7}$$

The corresponding boundary conditions will take the following form:

$$\begin{aligned} &f(0) = 0,\ f'(0) = A, \qquad \theta(0) = 1 \text{ at } \eta = 0, \\ &f'(\infty) = 1 - A, \quad \theta(\infty) = 0, \quad \text{as } \eta \to \infty \end{aligned} \tag{8}$$

where $A = \frac{U_w}{U_\infty}$ is the velocity ratio parameter, $Pr = \frac{(\mu c_p)_f}{k_f}$ is the Prandtl number, $Ec = \frac{{U_w}^2}{(T_w - T_\infty)c_{pf}}$ is the Eckert number and $R = \frac{16\sigma^* T_\infty^3}{3k_{nf}k^*}$ is the radiation parameter.

The physical quantities of interest are the skin friction coefficient (C_f) and the local Nusselt number (Nu_x), which are defined as:

$$C_f = \frac{\tau_w}{\rho_f U_w^2}, \qquad Nu_x = \frac{xq_w}{k_f(T_w - T_\infty)} \frac{\partial \mathrm{T}}{\partial \mathrm{y}}\bigg|_{y=0}$$

where the surface shear stress τ_w and the surface heat flux q_w are given by:

$$\tau_w = \mu_{nf}\left(\frac{\partial u}{\partial y}\right), \quad q_w = -k_{nf}\frac{\partial T}{\partial y} + (q_r)_w \quad \text{at } y = 0$$

with μ_{nf} and k_{nf} being the dynamic viscosity and thermal conductivity of the nanofluids, respectively. Using the similarity transformation equation (5), we obtain:

$$\sqrt{Re_x}C_f = \frac{1}{(1-\phi)^{2.5}} f''(0), \quad \frac{Nu_x}{\sqrt{Re_x}} = -\frac{k_{nf}}{k_f}\left(1 + R\theta^3{}_w\right)\theta'(0),$$

where $Re = \frac{U_\infty}{\nu_f}$ is the local Reynolds number.

Numerical method and code validation

The Runge–Kutta–Fehlberg fourth-fifth order method along with the shooting technique is used to solve the governing equations (6) and (7) with boundary conditions (8). A suitable finite value of η_∞ is considered in such a way that the boundary conditions are satisfied asymptotically. In addition, the relative error tolerance to 10^{-6} is considered for convergence, and the step size is chosen as $\Delta\eta = 0.001$. To examine the numerical procedure for validity and accuracy, the numerical results are compared with published work. The numerical code is validated with the benchmark results of Grubka and Bobba (1985), Chen (1998) at different Prandtl numbers as shown in Table I. In fact, excellent agreement is shown between the present results and the benchmark solutions (Tables II and III).

Table I. Comparison results for surface temperature gradient $[-\theta'(0)]$ in the case of $\phi = 0, R = 0, \theta_w = 0$ and $m = 0$

Pr	Grubka and Bobba (1985)	Chen (1998)	Present study
0.72	1.0885	1.0885	1.0884
1.0	1.3333	1.3333	1.3333
3.0	2.5097	2.5097	2.5096
10.0	4.7969	4.7968	4.7968

Table II. Thermophysical properties of Cu-water nanoparticles

	$\rho(kg/m^3)$	$C_p(j/kgk)$	$k(W/mk)$
H_2O	997.1	4,179	0.613
Cu	8,933	385	400

Result and discussion

To get a clear insight into the physical situation of the present problem, the numerical values for velocity and temperature profile are computed for different values of the dimensionless parameters using the method described in the previous section. The numerical results for the local skin friction coefficient and local Nusselt number are presented for different values of the governing parameters in Table IV. Figure 2 portrays the influence of ϕ on the $f'(\eta)$ field for the first and second solutions. In Figure 1, it is noticed that in the first solution (A = −0.1), the $f'(\eta)$ field increases by increasing the values of ϕ correspondingly increases the momentum boundary-layer thickness. But the second solution (A = −0.1) shows quite the opposite behavior.

A rise in the Pr increases the heat transfer rate in the surface of the fluid. This happens because increasing Pr increases the fluid viscosity but reduces the thermal conductivity, consequently increasing the heat transfer rate at the surface. This phenomenon is observed in Figure 3. Further, this figure reveals that the second solution shows the opposite behavior of the first solution.

Figure 4 displays the effect of R on the $\theta(\eta)$ field profile. It is noted that $\theta(\eta)$ increases with increasing values of R and correspondingly increases the thickness of the boundary layer. It is also noted that the maximum enhancement in the $\theta(\eta)$ profile is caused by the disk shape, followed by the needle- and sphere-shaped particles, respectively. Further, the disk-shaped particles requires maximum viscosity as compared to needle- and sphere-

Table III.
The value of parameters for thermal conductive and viscosity models

Nanoparticles	Shape factor (m)
Needle-shaped	4.9
Disc-shaped	8.6
Sphere-shaped	3

Table IV.
Numerical values of Nusselt number for different physical parameters with various shapes of nanoparticles

A	Ec	Pr	R	θ_w	ϕ(%)	Nusselt No. $m = 3$	$m = 4.9$	$m = 8.6$
0.2						0.36722	0.35144	0.32983
0.3						0.29671	0.29256	0.28353
0.4						0.21897	0.22635	0.23028
	0.1					0.33069	0.32112	0.30611
	0.2					0.29005	0.28739	0.27973
	0.3					0.24936	0.25364	0.25333
		5.776				0.35865	0.34247	0.32053
		6.587				0.36722	0.35151	0.32990
		7.578				0.37598	0.36090	0.33978
			0.5			0.36722	0.35144	0.32983
			1			0.33266	0.31642	0.29491
			1.5			0.30957	0.29332	0.27217
				1.2		0.36722	0.35144	0.32983
				1.4		0.32565	0.31078	0.29076
				1.6		0.28807	0.27416	0.25572
					1	0.43665	0.42492	0.40752
					2	0.36722	0.35144	0.32983
					3	0.30841	0.29212	0.27084

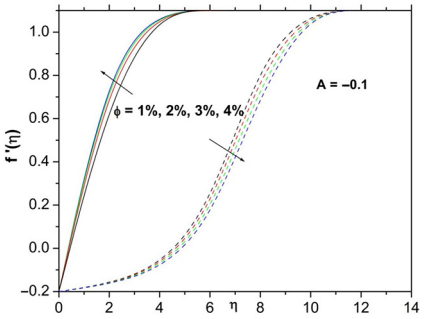

Figure 2.
Effect of ϕ on $f'(\eta)$

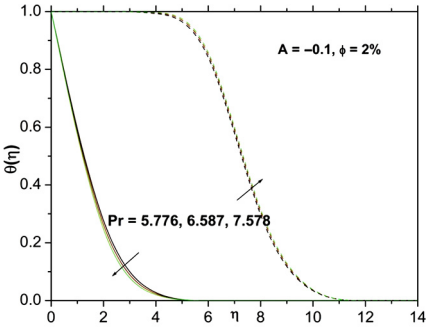

Figure 3.
Effect of Pr on $\theta(\eta)$

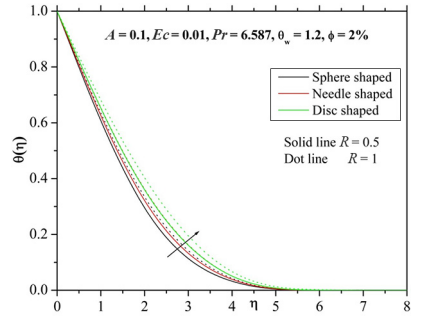

Figure 4.
Effect of R on $\theta(\eta)$

shaped particle-containing nanofluids. Figure 5 illustrates the effect of θ_w on $\theta(\eta)$. From the figure, as expected, we see that the $\theta(\eta)$ profile is higher for larger values of θ_w. Further, from this figure, we notice that the disk-shaped nanoparticles have higher temperature values than the needle- and sphere-shaped particles.

The effect of Ec on the $\theta(\eta)$ profile is highlighted in Figure 6. Here, the $\theta(\eta)$ and the corresponding thickness of the boundary layer increase by increasing values of Ec. The main reason for this effect is that the viscosity of the fluid takes energy from the motion of

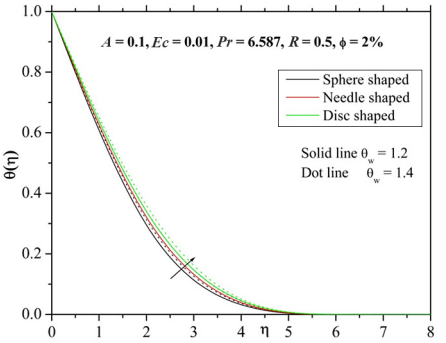

Figure 5.
Effect of θ_w on $\theta(\eta)$

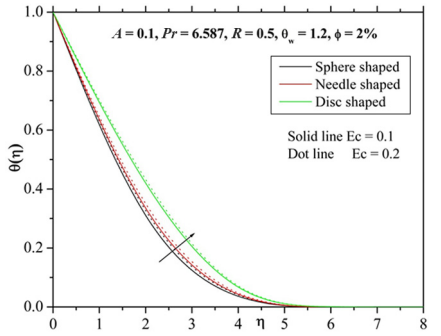

Figure 6.
Effect of Ec on $\theta(\eta)$

the fluid, transforming it into the internal energy of the fluid, which results in the heating of the fluid temperature. Hence, the thermal boundary layer thickens with the increase in viscous dissipation. Here, the disk-shaped nanoparticles have a higher temperature than the temperature of the needle- and sphere-shaped particles.

Figure 7 displays the effect of Pr on the Nusselt number. It is observed that the rate of heat transfer increases with increasing values of Pr. It is also observed that the thermal conductivity of the fluid is maximum because of the disk-shaped nanoparticles compared to other particle shapes. Figure 8 shows the influence of the A on the skin friction coefficient.

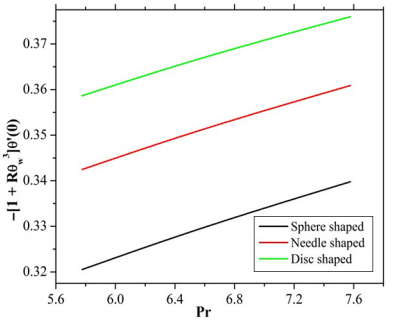

Figure 7.
Effect of Pr on Nusselt number

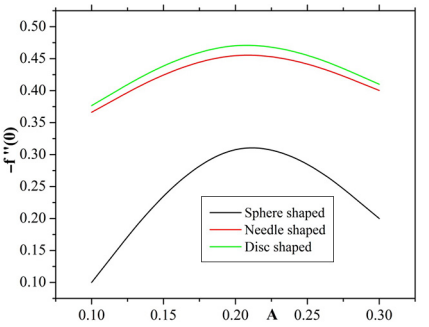

Figure 8.
Effect of A on skin friction coefficient

This figure reveals that higher values of A increase the skin friction coefficient. It is appropriate to mention here that the disk-shaped nanoparticles have the highest rate of skin friction coefficient at the surface, followed by the needle-shaped particles and, finally, the sphere-shaped particles, which have the lowest rate of skin friction coefficient at the wall.

Figure 9 shows the effect of variation of ϕ and A on the skin friction coefficient. It is noted that the skin friction coefficient decreases for larger values of ϕ and A. It is also noted that the maximum decrease in velocity is caused by the disk shape, followed by the needle- and sphere-shaped particles, respectively. This is in accordance with the physical expectation, a nanofluid containing disk-shaped particles requires maximum viscosity compared to needle- and sphere-shaped particles containing nanofluids.

Figure 10 shows the effects of θ_w and R on the skin friction coefficient. Here, we observe that the skin friction coefficient decreases for larger values of θ_w and R. Figure 11 delineates the influence of ϕ and Ec on the Nusselt number. We can observe from the figure that the Nusselt number decreases for larger values of ϕ and Ec. It can also be perceived from these figures that the maximum decrease in the rate of heat transfer is motivated by the disk-shaped particles, followed by the needle- and sphere-shaped particles. This is because the disk-shaped particles have maximum thermal conductivity compared to the other particle shapes. Table IV presents the numerical values of the Nusselt number for various values of the physical parameter. It is observed that the Nusselt number increases with increasing values of Pr. Furthermore,

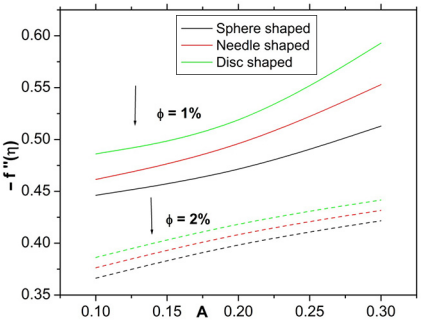

Figure 9.
Effect of ϕ and A on skin friction coefficient

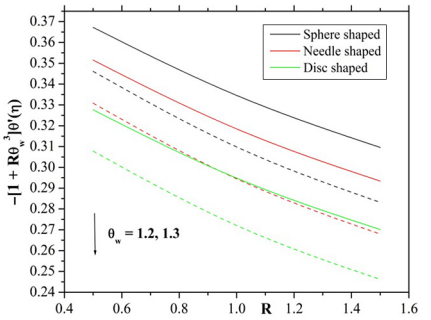

Figure 10.
Effect of θ_w and R on Nusselt number

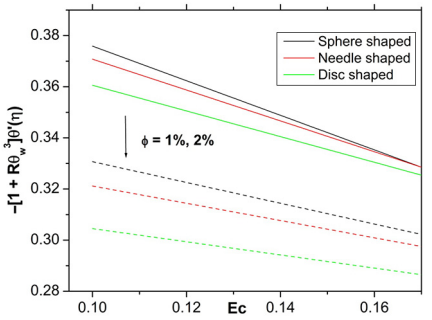

Figure 11.
Effect of ϕ and Ec on Nusselt number

from this table, we observe that the Nusselt number decreases with increasing values of θ_w, R, ϕ and A. Table V shows the numerical values of the skin friction coefficient and Nusselt number for the first and second solutions. From the table, one can infer that the first and second solutions show opposite behaviors.

Table V.
Numerical values of skin friction coefficient and Nusselt number with different parameters for both first and second solutions

Ec	Pr	ϕ(%)	First solution		Second solution	
			$\sqrt{Re_x}C_f$	$-\frac{Nu_x}{\sqrt{Re_x}}$	$\sqrt{Re_x}C_f$	$-\frac{Nu_x}{\sqrt{Re_x}}$
0.1			0.55369	0.40378	0.15624	0.19287
0.2			0.55369	0.30798	0.15624	0.39168
0.3			0.55369	0.21197	0.15624	0.59057
	5.776		0.55369	0.47797	0.15624	0.18370
	6.587		0.55369	0.48982	0.15624	0.14017
	7.578		0.55369	0.50200	0.15624	0.12537
		1	0.55369	0.48982	0.15896	0.13331
		2	0.54401	0.48199	0.15624	0.14017
		3	0.53440	0.47423	0.15353	0.14767

Conclusion

In this study, the nanoparticle shape effect on the thermophysical properties of a Cu-water nanofluid over a moving plate in the presence of nonlinear radiation and viscous dissipation has been examined. Some important features regarding the effects of different physical parameters on different flow fields of the problem are reported. The main outcomes are summarized as follows:

- The highlight of the study is that temperature profiles enhance more significantly in disk-shaped nanoparticles than needle- and sphere-shaped nanoparticles.
- Thermal boundary-layer thickness increases with increasing values of Ec and θ_w.
- The velocity profile enhances with larger values of ϕ in the first solution, but the opposite trend is found in the second solution.
- For larger values of Pr, the temperature profile decays.
- The rate of heat transfer increases by enhancing the values of R.

References

Bachok, N., Ishak, A. and Pop, I. (2010), "Boundary-layer flow of nanofluids over a moving surface in a flowing fluid", *International Journal of Thermal Sciences*, Vol. 49 No. 9, pp. 1663-1668.

Bachok, N., Ishak, A. and Pop, I. (2012), "Flow and heat transfer characteristics on a moving plate in a nanofluid", *International Journal of Heat and Mass Transfer*, Vol. 55 No. 4, pp. 642-648.

Cortell, R. (2014), "Fluid flow and radiative nonlinear heat transfer over a stretching sheet", *Journal of King Saud University-Science*, Vol. 26 No. 2, pp. 161-167.

Ellahi, R., Zeeshan, A. and Hassan, M. (2016), "Particle shape effects on Marangoni convection boundary layer flow of a nanofluid", *International Journal of Numerical Methods for Heat and Fluid Flow*, Vol. 26 No. 7, pp. 2160-2174.

Ellahi, R., Hassan, M., Zeeshan, A. and Khan, A.A. (2016), "The shape effects of nanoparticles suspended in HFE-7100 over wedge with entropy generation and mixed convection", *Applied Nanoscience*, Vol. 6 No. 5, pp. 641-651.

Grubka, L.J. and Bobba, K.M. (1985), "Heat transfer characteristics of a continuous stretching surface with variable temperature", *Journal of Heat Transfer*, Vol. 107 No. 1, pp. 248-250.

Gul, T., Khan, A.S., Islam, S., Alqahtani, A.M., Khan, I., Alshomrani, A.S. and Alzahrani, A.K. (2017), "Heat transfer investigation of the unsteady thin film flow of Williamson fluid past an inclined and oscillating moving plate", *Applied Sciences*, Vol. 7 No. 4, p. 369.

Hayat, T., Muhammad, T., Alsaedi, A. and Alhuthali, M.S. (2015), "Magnetohydrodynamic three-dimensional flow of viscoelastic nanofluid in the presence of nonlinear thermal radiation", *Journal of Magnetism and Magnetic Materials*, Vol. 385, pp. 222-229.

Hayat, T., Qayyum, S., Shehzad, S.A. and Alsaedi, A. (2017), "Simultaneous effects of heat generation/absorption and thermal radiation in magnetohydrodynamics (MHD) flow of Maxwell nanofluid towards a stretched surface", *Results in Physics*, Vol. 7, pp. 562-573.

Hussain, S.M., Jain, J., Seth, G.S. and Rashidi, M.M. (2017), "Free convective heat transfer with hall effects, heat absorption and chemical reaction over an accelerated moving plate in a rotating system", *Journal of Magnetism and Magnetic Materials*, Vol. 422, pp. 112-123.

Kadiyala, P.K. and Chattopadhyay, H. (2018), "Numerical analysis of heat transfer from a moving surface due to impingement of slot jets", *Heat Transfer Engineering*, Vol. 39 No. 2, pp. 98-106.

Khan, M., Irfan, M. and Khan, W.A. (2017), "Impact of nonlinear thermal radiation and gyrotactic microorganisms on the Magneto-Burgers nanofluid", *International Journal of Mechanical Sciences*, Vol. 130, pp. 375-382.

Kumar, K.G., Ramesh, G.K. and Gireesha, B.J. (2018), "Impact of thermal radiation on double-diffusive natural convection flow of MHD casson fluid past a stretching vertical surface", *Frontiers in Heat and Mass Transfer (FHMT)*, Vol. 9 No. 1.

Kumar, R., Sood, S., Sheikholeslami, M. and Shehzad, S.A. (2017), "Nonlinear thermal radiation and cubic autocatalysis chemical reaction effects on the flow of stretched nanofluid under rotational oscillations", *Journal of Colloid and Interface Science*, Vol. 505, pp. 253-265.

Lin, Y., Li, B., Zheng, L. and Chen, G. (2016), "Particle shape and radiation effects on Marangoni boundary layer flow and heat transfer of copper-water nanofluid driven by an exponential temperature", *Powder Technology*, Vol. 301, pp. 379-386.

Ma, J., Sun, Y. and Li, B. (2017), "Spectral collocation method for transient thermal analysis of coupled conductive, convective and radiative heat transfer in the moving plate with temperature dependent properties and heat generation", *International Journal of Heat and Mass Transfer*, Vol. 114, pp. 469-482.

Makinde, O.D. and Animasaun, I.L. (2016), "Bioconvection in MHD nanofluid flow with nonlinear thermal radiation and quartic autocatalysis chemical reaction past an upper surface of a paraboloid of revolution", *International Journal of Thermal Sciences*, Vol. 109, pp. 159-171.

Ooi, E.H. and Popov, V. (2013), "Numerical study of influence of nanoparticle shape on the natural convection in Cu-water nanofluid", *International Journal of Thermal Sciences*, Vol. 65, pp. 178-188.

Ramesh, G.K., Gireesha, B.J. and Bagewadi, C.S. (2012), "Stagnation point flow of a MHD dusty fluid towards a stretching sheet with radiation", *Afrika Matematika*, Vol. 25 No. 1, pp. 237-249.

Ramesh, G.K., Gireesha, B.J. and Gorla, R.S.R. (2015), "Study on Sakiadis and Blasius flows of Williamson fluid with convective boundary condition", *Nonlinear Engineering*, Vol. 4 No. 4, pp. 215-221.

Ramesh, G.K., Roopa, G.S., Gireesha, B.J., Shehzad, S.A. and Abbasi, F.M. (2017), "An electro-magneto-hydrodynamic flow Maxwell nanoliquid past a Riga plate: a numerical study", *Journal of the Brazilian Society of Mechanical Sciences and Engineering*, Vol. 39 No. 11, pp. 4547-4554.

Rauf, A., Shehzad, S.A., Hayat, T., Meraj, M.A. and Alsaedi, A. (2017), "MHD stagnation point flow of micro nanofluid towards a shrinking sheet with convective and zero mass flux conditions", *Bulletin of the Polish Academy of Sciences Technical Sciences*, Vol. 65 No. 2, pp. 155-162.

Rudraswamy, N.G., Kumar, K.G., Gireesha, B.J. and Gorla, R.S.R. (2016), "Soret and Dufour effects in three-dimensional flow of Jeffery nanofluid in the presence of nonlinear thermal radiation", *Journal of Nanoengineering and Nanomanufacturing*, Vol. 6 No. 4, pp. 278-287.

Shehzad, S.A., Hayat, T., Alsaedi, A. and Mustafa, A.O. (2014), "Nonlinear thermal radiation in three-dimensional flow of Jeffrey nanofluid: a model for solar energy", *Applied Mathematics and Computation*, Vol. 248, pp. 273-286.

Sheikholeslami, M. and Shehzad, S.A. (2017), "Thermal radiation of ferrofluid in existence of Lorentz forces considering variable viscosity", *International Journal of Heat and Mass Transfer*, Vol. 109, pp. 82-92.

Sheikholeslami, M. and Shehzad, S.A. (2018), "Numerical analysis of Fe_3O_4-H_2O nanofluid flow in permeable media under the effect of external magnetic source", *International Journal of Heat and Mass Transfer*, Vol. 118, pp. 182-192.

Sheikholeslami, M., Shehzad, S.A., Li, Z. and Shafee, A. (2018), "Numerical modeling for alumina nanofluid magnetohydrodynamic convective heat transfer in a permeable medium using Darcy law", *International Journal of Heat and Mass Transfer*, Vol. 127, pp. 614-622.

Timofeeva, E.V., Routbort, J.L. and Singh, D. (2009), "Particle shape effects on thermophysical properties of alumina nanofluids", *Journal of Applied Physics*, Vol. 106 No. 1, pp. 014304.

Trodi, A. and Hocine Benhamza, M.E. (2016), "Particle shape and aspect ratio effect of Al_2O_3-water nanofluid on natural convective heat transfer enhancement in differentially heated square enclosures", *Chemical Engineering Communications*, Vol. 204 No. 2, pp. 158-167.

Turkyilmazoglu, M.M. (2013), "Unsteady convection flow of some nanofluids past a moving vertical flat plate with heat transfer", *Journal of Heat Transfer*, Vol. 136 No. 3, pp. 031704-031707.

Upadhya, S.M., Ramesh, G.K. and Makinde, O.D. (2018), "MHD flow of dusty fluid past a stretching sheet with slip effect using carreau model", *Defect and Diffusion Forum*, Vol. 387, pp. 135-144.

Waqas, M., Hayat, T., Shehzad, S.A. and Alsaedi, A. (2018), "Transport of magnetohydrodynamic nanomaterial in a stratified medium considering gyrotactic microorganisms", *Physica B: Condensed Matter*, Vol. 529, pp. 33-40.

Xie, H.Q., Wang, J.C., Xi, T.G., Liu, Y., Ai, F. and Wu, Q.R. (2012), "Thermal conductivity enhancement of suspensions containing nanosized alumina particles", *Journal of Applied Physics*, Vol. 91 No. 7, pp. 4568-4572.

Further reading

Chen, C.H. (1998), "Laminar mixed convection adjacent to vertical, continuously stretching sheets", *Heat and Mass Transfer*, Vol. 33 Nos 5/6, pp. 471-476.

Corresponding author

Ganesh Kumar K. can be contacted at: ganikganesh@gmail.com